Title

Stability of tropical forest tree carbon-water relations in a rainfall exclusion treatment through shifts in effective water uptake depth

Journal

Global Change Biology, 27(24)

ISSN

1354-1013

Authors

Pivovaroff, Alexandria L

McDowell, Nate G

Rodrigues, Tayana Barrozo

et al.

Publication Date

2021-12-01

DOI

10.1111/gcb.15869

Peer reviewed

DR. ALEXANDRIA PIVOVAROFF (Orcid ID : 0000-0002-3104-1900)
DR. NATE MCDOWELL (Orcid ID : 0000-0002-2178-2254)
MS. TAYANA BARROZO RODRIGUES (Orcid ID : 0000-0002-3174-0533)
DR. LUCAS A. CERNUSAK (Orcid ID : 0000-0002-7575-5526)
DR. KOLBY JARDINE (Orcid ID : 0000-0001-8491-9310)
DR. SUSAN G. W. LAURANCE (Orcid ID : 0000-0002-2831-2933)
DR. WEIBIN LI (Orcid ID : 0000-0001-8970-0318)
DR. JEN PETERS (Orcid ID : 0000-0003-4627-7788)

Article type : Primary Research Article

Stability of tropical forest tree carbon-water relations in a rainfall exclusion treatment through shifts in effective water uptake depth

Running title: Tropical trees shift depth of water uptake

Authors

Alexandria L. Pivovaroff[1,*], Nate G. McDowell[1,2], Tayana Barrozo Rodrigues[3], Tim Brodribb[4], Lucas A. Cernusak[5], Brendan Choat[6], Charlotte Grossiord[7,8], Yoko Ishida[5], Kolby J. Jardine[9], Susan Laurance[5], Riley Leff[1], Weibin Li[1, 10], Michael Liddell[5], D. Scott Mackay[11], Heather Pacheco[1], Jennifer Peters[6,12], Israel de J. Sampaio Filho[3], Daisy C. Souza[3], Wenzhi Wang[1], Peipei Zhang[1], Jeff Chambers[13]

Affiliations

[1]Atmospheric Science and Global Change Division, Pacific Northwest National Laboratory, Richland, WA, USA

[2]School of Biological Sciences, Washington State University, Pullman, WA, USA

[3]Forest Management Laboratory, National Institute of Amazonian Research, Manaus, Amazonas, Brazil

[4]School of Biological Sciences, University of Tasmania, Hobart, TAS 7001, Australia

[5]College of Science and Engineering, James Cook University, Cairns, Queensland, Australia

[6]University of Western Sydney, Hawkesbury Institute for the Environment, Richmond, New South Wales 2753, Australia

[7]Plant Ecology Research Laboratory, School of Architecture, Civil and Environmental Engineering, EPFL, Lausanne, Switzerland

[8]Functional Plant Ecology, Community Ecology Unit, Swiss Federal Institute for Forest, Snow and Landscape Research (WSL), Lausanne, Switzerland

[9]Climate and Ecosystem Sciences Division, Lawrence Berkeley National Laboratory, Berkeley, CA, USA

[10]State Key Laboratory of Grassland and Agro-ecosystems, Key Laboratory of Grassland Livestock Industry Innovation, Ministry of Agriculture and Rural Affairs, College of Pastoral Agriculture Science and Technology, Lanzhou University, Lanzhou 730020, China

[11]Department of Geography and Department of Environment & Sustainability, University at Buffalo, Buffalo, NY, USA

[12]Oak Ridge National Laboratory, Climate Change Science Institute & Environmental Science Division, P.O. Box 2008, Oak Ridge, TN 37831 USA.

[13]Climate Sciences Department, Earth Sciences Division, Lawrence Berkeley National Laboratory, Berkeley, CA 94720

*Corresponding author
Email: alexandria.pivovaroff@pnnl.gov
Phone: +1 562 881 4640

Abstract

Increasing severity and frequency of drought is predicted for large portions of the terrestrial biosphere, with major impacts already documented in wet tropical forests. Using a four-year rainfall exclusion experiment in the Daintree Rainforest in northeast Australia, we examined canopy tree responses to reduced precipitation and soil water availability by quantifying seasonal changes in plant hydraulic and carbon traits for 11 tree species between control and drought treatments. Even with reduced soil volumetric water content in the upper 1m of soil in the drought treatment, we found no significant difference between treatments for predawn and midday leaf water potential, photosynthesis, stomatal conductance, foliar stable carbon isotope composition, leaf mass per area, turgor loss point, xylem vessel anatomy, or leaf and stem non-structural carbohydrates. While empirical measurements of above-ground traits revealed homeostatic maintenance of plant water status and traits in response to reduced soil moisture, modeled below-ground dynamics revealed that trees in the drought treatment shifted the depth from which water was acquired to deeper soil layers. These findings reveal that below-ground acclimation of tree water uptake depth may buffer tropical rainforests from more severe droughts that may arise in the future with climate change.

Keywords

Plant hydraulics, non-structural carbohydrates, water potentials, drought, wet tropical forest, turgor loss point, gas exchange, rainfall exclusion, rooting depth, process model

Introduction

Drought can push ecosystems beyond thresholds of vulnerability (Crausbay et al., 2017), and is expected to become more frequent, intense, widespread, and last longer under future conditions due to Earth's warming atmosphere (Trenberth et al., 2014). This has global implications because drought is a major driver of forest mortality worldwide (McDowell et al., 2020). Forest mortality has negative consequences for biogeochemical cycles and biodiversity. In moist tropical forests, tree mortality rates have generally increased in recent decades due to climate change, as observed in the Amazon Basin (Brienen et al., 2015; Hubau et al., 2020), Southeast Asia (Phillips et al., 2010), and the Congo (Zhou et al., 2014, but see Hubau et al., 2020). However, geographic differences in drought-induced forest mortality rates contribute to the difficulty in explaining the mechanisms underlying tree mortality and predicting future responses.

Loss of hydraulic function, depletion of non-structural carbon stores, and biotic disturbance all contribute to tree mortality, often in combination (McDowell et al., 2011). Hydraulic failure is associated with the vascular system of plants becoming increasingly air-filled due to cavitation, as the water status of the plant exceeds critical thresholds of hydraulic safety (Choat et al., 2018). High levels of embolism prevent water movement from the roots through the shoots and to the leaves, ultimately leading to desiccation. As part of the drought response sequence, plants close their stomata to maintain their water status and delay the onset of cavitation. As a result, plants shift their carbon metabolism as the photosynthetic uptake of carbon is reduced, and plants may begin to deplete non-structural stores of carbon. The continued metabolic demand for carbohydrates, along with the interaction of desiccation, can push plants to an unrecoverable point, ultimately resulting in death (Hammond et al., 2019). While we have a good knowledge of these above-ground processes and their role in tree mortality, we have limited knowledge of below-ground processes, particularly in the tropics.

Predicting drought impacts on tree function is especially difficult in moist tropical forests due to limited field data and the poor representation of processes controlling biogeochemical processes in the tropics in Earth system models (Patrick Meir et al., 2015; Patrick Meir & Woodward, 2010). This is of particular concern because of the ecological value of moist tropical forests and their role in global processes, such as carbon and water cycles. Experimental drought manipulation studies can be

a valuable tool in understanding the effects of drought and mechanisms of drought mortality in moist tropical forests (da Costa et al., 2010; P. Meir et al., 2009). However, implementing large-scale rainfall exclusion experiments is difficult, and therefore, these types of studies in tropical forests are limited. Two throughfall exclusion experiments include Caxiuanã and Tapajós National Forest Reserves, which are both in the Amazon rain forest of Brazil. Examining additional forests, especially ones with narrow hydraulic safety margins (Peters et al., 2021), is necessary to further understand tropical tree responses to drought and long-term risk or resilience of moist tropical forests.

Process-based models are an essential tool for understanding and predicting ecological processes and responses to environmental conditions (Cuddington et al., 2013). For example, they can provide mechanistic insight into drought responses and mortality variability among species (Johnson et al., 2018). The "Sperry" model" (Sperry et al., 2016, 2017; Sperry & Love, 2015; Venturas et al., 2018) is a robustly tested model that can be highly constrained by field observations, thus enabling the generation of highly accurate results. As above-ground traits tend to be measured more frequently than below-ground traits, these models can be highly constrained to also investigate below-ground dynamics (Love et al., 2019), including rooting depth. Rooting depth and the depth from which water is acquired are critical for plant responses to drought (Johnson et al., 2018; Poyatos et al., 2018). Tree below-ground dynamics can shift seasonally with rainfall (Barbeta et al., 2015; Klein et al., 2014; Snyder & Williams, 2003; Voltas et al., 2015), with water access helping to mitigate the effects of heat waves and drought (David et al., 2007; Eggemeyer et al., 2009; Rossatto et al., 2012). Below-ground dynamics are important for plant water acquisition and response to drought and can play an important role in explaining why some trees succumb to drought while others survive, and models can be used to fill in this key gap.

Our objective was to test the impacts of drought on changes in plant hydraulic and carbon traits in the context of tree mortality in a moist tropical forest. Utilizing a four-year rainfall exclusion experiment at the Daintree Rainforest Observatory in Australia, we empirically measured above-ground plant hydraulic traits including predawn and midday leaf water potential, turgor loss point, stomatal conductance and water use efficiency, in canopy trees in the control and drought treatment. As soil volumetric water content is reduced in the drought treatment, especially in the upper soil layers (Figure 1) (Tng et al., 2018), we hypothesized that:

1) Droughted trees would have more negative water potentials than non-droughted trees.
2) Foliar turgor loss point would shift to be more negative in the drought treatment.
3) Water constraints (determined from soil volumetric water content and leaf water potential) would reduce photosynthesis and stomatal conductance in droughted trees compared to non-droughted trees.
4) Trees in the drought treatment would shift hydraulic anatomy, having both smaller and fewer vessels.
5) Carbohydrates would be lower in droughted trees than non-droughted trees.

We then used these field-collected data to parameterize a process-based photosynthetic gain and hydraulic cost optimization model (Sperry et al., 2017; Venturas et al., 2018) to investigate below-ground dynamics, including the effective depth of water uptake in the control and drought trees. We hypothesized that:

6) Drought trees would shift their effective water uptake depth to deeper layers than non-droughted trees.

Materials & Methods

Study site

The study was conducted in a lowland tropical rainforest at the Daintree Rainforest Observatory (DRO; 16°06′20″S 145°26′40″E, 50 m a.s.l.) adjacent to the Daintree National Park in north-eastern Australia. The Daintree Rainforest in Australia is the oldest continually surviving tropical rainforest in the world and is listed as a UNESCO World Heritage site. The mean temperature is 24.4°C, and the average annual rainfall is 5143mm/year (TERN, 2020). There is a distinct wet season with the majority of rainfall occurring from December to April (Figure 1).

At the DRO, there is a 1-ha long-term forest monitoring plot with a 47m tall crane with a 55m arm that allows access to the forest canopy. Within this plot, an *in-situ* drought experiment was established in May 2015, consisting of two rainfall exclusion structures each covering 2000m^2 rectangular patches of the monitoring plot. The rainfall exclusion structures are made of clear-panel roofing that is sloped, directing intercepted rain into aluminum troughs that carry the intercepted rainwater away from the plot. Leaf litter that falls on the roof of the structures or in the troughs is

transferred back to the soil surface. The area of the 1 ha forest census plot at the base of the crane (Laidlaw et al., 2007) not covered by the rainfall exclusion structures is considered the control treatment.

Soil volumetric water content (SVWC) was measured with soil moisture sensors installed in soil pits. Four pits are in the control treatment and four pits are in the drought treatment, for a total of eight pits. Within each pit, time domain reflectometry probes (CS616, Campbell Scientific, UK) are installed at four soil depths, 10, 50, 100, and 150 cm, to log soil moisture continuously (Figure 1).

Eleven canopy-dominant tree species were selected that had maximum light exposure. Tree size was controlled for as much as possible for species between drought and control individuals. We sampled one individual in the control plot and one individual in the drought plot (n = 22) for each species. The study species were: *(1) Castanospermum australe,* (2) *Cleistanthus myrianthus,* (3) *Cryptocarya mackinnoniana,* (4) *Dysoxylum papuanum*, (5) *Elaeocarpus angustifolius (Elaeocarpus grandis),* (6) *Endiandra microneura,* (7) *Mallotus paniculatus, (8) Myristica globosa, (9) Rockinghamia angustifolia*, (10) *Synima cordierorum,* (11) *Syzygium spp.* This level of replication among species rather than within species was aimed at capturing the community response rather than individual species responses and was also necessary because we were limited in access to multiple individuals of a species due to the footprint/access of the canopy crane.

Data were collected in November 2018, to sample the end of the dry season when soil volumetric water content is lowest and the difference in soil moisture between treatments is smallest, and again in May 2019, to sample the end of the wet season when soil volumetric water content is high and the difference in soil moisture between treatments is greatest, in order to examine peak differences between control and drought treatment after ~4 years of experimental drought exposure.

Gas exchange

We measured diurnal leaf-level gas exchange with a portable photosynthesis system (LI-6800, LI-COR Inc., Lincoln, NE, USA) using the clear-top 3 × 3 cm leaf chamber and light source. To control for changing ambient conditions between measurements over time, we always measured the same species in one treatment immediately followed by the same species in the other treatment (versus measuring all species in the control and then measuring all the species in the drought treatment).

During the dry season, we measured a minimum of six leaves per tree per treatment. During the wet season, a cyclone produced high wind conditions that limited the safe use of the canopy crane, so we measured a minimum of one leaf per tree per treatment. Photosynthetically active radiation (PAR) was set to 1000 μmol m^{-2} s^{-1}, reference CO_2 was set to 420 μmol mol^{-1}, temperature was kept close to ambient and from about 29°C to 32°C, and relative humidity was kept close to ambient (this varied between 40 to 80%). Large branches were cut from the tree and placed in a bucket of water, after which time we immediately measured gas exchange of sunlit, healthy, recently expanded mature leaves while the gondola concurrently moved to the next target tree. Leaves were large and fully covered the chamber. Measurements were recorded every 3 seconds for a 3 minute period, and we took the average of the entire 3 minutes. We determined photosynthesis (A;μmol m^{-2} s^{-1}), stomatal conductance (g_s; mol m^{-2} s^{-1}) and intrinsic water use efficiency as photosynthesis divided by stomatal conductance (A/g_s).

Water potentials

Leaf water potentials (Ψ; MPa) were measured using a Scholander-type pressure chamber (PMS Instrument Co., Albany, OR, USA). Upon cutting a large branch for gas exchange (see above), a terminal leaf or small shoot was sub-sampled for water potential measurement. These samples were immediately sealed in a plastic bag and transported from the crane gondola to the ground. Leaf water potential was measured at predawn (Ψ_{PD}) and midday (Ψ_{MD}). During the dry season, we measured a minimum of six leaves per tree per treatment. During the wet season, a cyclone produced high wind conditions that limited the safe use of the canopy crane, so we measured a minimum of one leaf per tree per treatment.

Pressure volume curves

In November, pressure volume curves were determined on three terminal shoots per species per treatment using the bench-dehydration method. Branches were sampled from the canopy, placed in large buckets of water, and transported to the lab. In the lab prior to measurement, leaves were cut from the branches and then immediately weighed for mass. Leaves were subsequently measured for water potential using a Scholander-type pressure chamber (Model 1505D pressure chamber, Plant

Moisture Stress Instruments, Albany, OR, USA), followed by a period of dehydration. This was repeated, with dehydration times increasing with each round, until achieving a water potential of about −4 MPa or until leaves were visibly wilted, depending on the species. Subsequently, samples were put in a paper bag and dried in an oven at 70°C for at least 48 h to determine dry mass. We calculated saturated water content (*SWC*; %), water potential at turgor loss point (Ψ_{TLP}; MPa), relative water content at turgor loss point (RWC_{TLP}; %), osmotic potential (π_o; MPa), modulus elasticity (ε; MPa), capacitance at full turgor (C_{FT}; MPa^{-1}), capacitance at turgor loss point (C_{TLP}; MPa^{-1}), and leaf dry matter content (*LDMC*; $g\ g^{-1}$) (Vargas, 2019).

Wood anatomy

During each sampling campaign, we cut a 20 cm-long stem sample (approx. 70 cm from the apex, diameter between 2-3 cm) from the top of each tree's canopy to determine wood anatomical properties. The samples were stored in plastic vials with a 50% Ethanol solution until further laboratory analyses. Transversal sections of each sample (20 µm thick) were made with a Leica microtome and stained with Safranin-O and Astra blue (1% and 0.5% in distilled water, respectively). The sections were mounted on glass slides with a coverslip. Microscopic digital images were captured at 20x magnification with a compound microscope (BX51, Olympus, Germany) interfaced with a Canon camera (Canon EOS 1200D, Switzerland). Digital images were taken on a radial path from the pith to the bark. Image analyses were performed with the ImageJ software. The total number of vessels and the lumen area (µm) were measured on the last two growth rings, as these vessels are responsible for the majority of water transport (Bouche et al., 2014; Domec & Gartner, 2002). Vessel density (vessels cm^{-2}) was calculated by dividing the number of vessels by the area measured.

Leaf mass per area and stable isotopes

We used a cork borer with a known inner diameter to take two punches from three different leaves for each tree, avoiding the mid-vein when possible. These leaf punches were placed in a coin envelope and dried in an oven at 65°C for more than 48h. After this, the dry weight was determined using an analytical balance. Leaf mass per area ($g\ cm^{-2}$) was determined as the fresh leaf area (known from the size the leaf punches and the number of leaf punches) divided by the dry mass.

To analyze the stable carbon isotope composition ($\delta^{13}C$) and percent carbon, we collected an additional two punches from three different leaves for each tree, placed them in coin envelopes, oven dried them at 65°C for more than 48 h. After this, samples were ground to a consistent particle size, weighed, and put in tin capsules before being shipped in a secured 96 position cell plate to the Stable Isotope Core facility at Washington State University for percent carbon and $\delta^{13}C$ analysis with an Elemental Analyzer - Isotope Ratio Mass Spectrometer (EA-IRMS; Delta XP, Thermo Scientific). Final $\delta^{13}C$ content values are expressed relative to international standard Vienna Pee Dee belemnite (V-PDB) for carbon; $\delta^{13}C$ of plant tissues can provide a measure of integrated water use efficiency when carbon was assimilated, giving a time-integrated measure to complement instantaneous measurements. For a subset of five species (*C. australe, C. myrianthus, D. papauanum, M. globosa, S. graveolens*), we were able to sample leaves from at least three individuals per treatment to test for within-species differences in $\delta^{13}C$ between treatments.

Non-structural carbohydrates

Non-structural carbohydrates (NSC) of leaf punches, twigs, and tree cores were analyzed. NSCs were defined as free, low molecular weight sugars (glucose, fructose, and sucrose) plus starch. Within 2 hours of collection, all samples were microwaved at 800W for 90 sec to stop enzymatic activity, then placed in coin envelopes and dried in the drying oven at 65°C for 72 h. After this, samples were kept dry until being ground to fine powders (Landhäusser et al., 2018). We followed the detailed protocol described by (Hoch et al., 2002) with the ethanol extraction modification from (Landhäusser et al., 2018), described more briefly here. After being ground to a fine powder, samples were extracted three times with 80% ethanol at 90°C. The supernatant obtained after centrifuge was used for soluble sugar quantification (i.e glucose, fructose and sucrose) via enzymatic assay. To determine sugar concentrations, sucrose was broken down to glucose and fructose by invertase (Sigma cat. no. I9274), while glucose and fructose were phosphorylated to glucose-6-phosphate by hexokinase (Sigma cat. no. G3293) with isomerase (Sigma cat. no. P5381-5KU). Glucose-6-phosphate concentration was determined photometrically in a 96-well microplate reader (ELx800UV, BioTek Instruments, Winooski, USA) by measuring the increase in absorbance at 340 nm as NAD+ was reduced to NADH, with glucose of known concentrations as standards. The ethanol-insoluble residual separated

after extraction was used for starch digestion after ethanol evaporation. Starch in the pellet was hydrolyzed to water soluble glucans using α-amylase from Bacillus licheniformis (Sigma cat. no. A4551). After removal of structural carbohydrates by centrifuge, the glucans contained in the supernatant were hydrolyzed into glucose by amyloglucosidase from Aspergillus niger (Sigma cat. no. ROAMYGLL). Two inter-lab standards (peach leaves NIST1547 and pinon needles) and one synthetic standard (Landhäusser et al., 2018) were also applied in the analyses. The glucose hydrolysate was quantified as the glucose quantification above. Starch concentration was calculated by multiplying the glucose hydrolysate concentration by a conversion factor of 0.9. The total NSC was calculated as the sum of starch and soluble sugar concentrations as percentage of dry matter (% dry matter).

Abscisic acid

We measured foliar abscisic acid (ABA) concentrations to assess if stomatal regulation was influenced differently by ABA between the treatments. For each species in each treatment, leaves were collected from the canopy. In the gondola, the leaves were immediately processed to sample two leaf discs from each of three different leaves using a cork borer, avoiding the mid-vein when possible. These samples were placed in coin envelopes and then into a liquid nitrogen dry shipper in the gondola. In the lab, the six frozen leaf discs were removed from the coin envelope and placed in a vial with 5 mL of methanol, which was then covered with parafilm, closed, and stored in a refrigerator at 5°C. Then, the tissue samples were homogenized and ABA was extracted, purified, and quantified following the detailed protocol of (McAdam, 2015) and (McAdam & Brodribb, 2014).

Modeling approach

We used a photosynthetic gain and hydraulic cost optimization model (Sperry et al., 2017; Venturas et al., 2018) run at hourly time steps from May 2018 to August 2019 to assess how tree effective water acquisition depth may have shifted between the control and drought treatments for each species. The original model code was ported into R (version 4.0.2) and run using the 'ezsperry' package (Leff, 2020) in R Studio (version 1.3.1073) (R Core Team, 2020; RStudio Team, 2020). The model was forced with hourly meteorological observations including precipitation, air temperature, solar

radiation, atmospheric vapor pressure deficit, and wind speed, which were measured at the study site with a weather transmitter (WXT520, Vaisala, Helsinki, Finland) mounted on the load-jib on the crane, about 47m off the ground. For a data gap from January to June 2019, we used observations from a nearby weather station at Cow Bay (16.23819° S, 145.427151° E). The model was then parameterized with stand, soil, plant, photosynthetic, atmospheric, and vulnerability curve measurements, which are described along with units, values, and references in Supplemental Table 1 further laid out next in the text.

Measured site values used to parameterize the model included latitude, longitude, elevation, canopy leaf area index (Liddell & Laurance, 2015), and basal area to ground area ratio (Tng et al., 2016). Measured soil parameters included the fraction of rock in the soil, van Genuchten parameters α and *n* (van Genuchten, 1980) based on the texture of each soil layer (Liddell, 2015) (Supplemental Table 2 and Supplemental Figure 1). Leaf area to basal area was kept at the default value of 1000 m^2 m^{-2}. Measured parameters included tree height, maximum carboxylation rate at 25°C (V_{max25}), and maximum electron transport rate at 25°C (J_{max25}). To determine V_{max25} and J_{max25}, one branch per species per plot was cut from the canopy and placed in a bucket of water and returned to the ground for measurement of a CO_2 response (A-C_i) curve. The photosynthesis model of (Farquhar & von Caemmerer, 1980) was fitted to the A-C_i curves using the 'Plantecophys' package in R (R. A. Duursma, 2015). Hydraulic vulnerability curves were measured at the site for eight of the study species using the benchtop dehydration method; full curves and methods can be found in (Peters et al., 2021). The water potential at 50% loss of hydraulic conductivity (P_{50}) was calculated using the 'fitplc' package (R. Duursma & Choat, 2017) in R v.3.2.0 and these values were used to derive vulnerability curve parameters including Weibull function curve parameters *b* and *c*. The remaining 3 species were not conducive to hydraulic measurements due to excessive latex and mucilage in the stems and thus were excluded from the modeling component of the study.

In the model, root layer depths are based on the function:

$$B = 1 - \beta^d$$

Which assumes equal root biomass in each soil layer, where B is the fraction of root biomass above depth d in cm, with the β coefficient between 0 and 1. Essentially, β determines root layer depths based on a given number of total layers (Supplemental Figure 2). To assess how the effective water

uptake depth shifted between the control and drought treatments for each species, we manipulated β. We tested β from 0.960 to 0.995, which corresponds to maximum effective water uptake depths of 1.30m to 10.57m, in increments of 0.001 to determine the lowest β and therefore the shallowest depth of effective water uptake possible for each species in each treatment before minimum seasonal water potentials became too low, causing catastrophic cavitation and subsequently reduced transpiration. A benchmark analysis demonstrating the sensitivity of our simulation to β is shown in Supplemental Figure 3, demonstrating that changing β had a significant impact on the model outputs and that a uniform β was not appropriate across all species and treatments. Model output results were validated against predawn and midday water potentials and photosynthesis from the November field campaign (Supplemental Figure 4).

Statistics

All statistical tests were done in R (version 4.0.2) using R Studio (version 1.3.1073) (R Core Team, 2020; RStudio Team, 2020). We first tested for differences in soil volumetric water content between treatments using a linear mixed effects model with the 'lmer' function from the 'lme4' package in R; treatment, depth, and month were fixed effects while pit number was a random effect. Linear mixed effects models were also used to test for differences between treatments and seasons for predawn and midday water potential, photosynthesis, stomatal conductance, intrinsic water use efficiency (A/g_s), leaf mass per area, $\delta^{13}C$, and ABA; treatment and season were fixed effects, while species was a random effect. To test for differences in pressure volume curve traits between treatments, we used a multivariate analysis of variance (MANOVA) with the 'manova' function in the 'stats' package. We also used MANOVA to test for differences in vessel anatomy, specifically mean vessel area per mm^2 and number of vessels per mm^2, between treatments and months. The effects of treatments, months, and tissues on concentrations of NSC and its components were also tested by MANOVA. To test for within-species differences in $\delta^{13}C$ between treatments for the subset of 5 species with n=3 trees per treatment, we used analysis of variance (ANOVA) with the 'aov' function in the 'stats' package. To test if β and rooting depth from the model results shifted between the control and drought treatment, we used an ANCOVA to compare the intercept and slope of the control versus drought linear regression to a 1:1 line.

Results

Soil volumetric water content was significantly lower in the drought versus control treatment ($p < 0.05$; Figure 1). Predawn water potentials were less negative than midday water potentials ($p < 0.0001$), but there was no significant difference in predawn or midday water potentials between treatments ($p = 0.33$) or months ($p = 0.17$; Figure 2). Photosynthesis and stomatal conductance were both higher in May compared to November ($p < 0.0001$), but there were no differences between treatments ($p = 0.19$; Figure 2). While there was a difference in intrinsic water use efficiency (A/g_s) between treatment ($p < 0.0001$) and months ($p < 0.0001$) (Figure 2), there was no significant difference in $\delta^{13}C$, which is a measure of integrated water use efficiency, between treatment ($p = 0.83$) or months ($p = 0.41$; Figure 3). Further, in testing for within-species differences in foliar $\delta^{13}C$ between treatments for a subset of 5 species, there were no differences between treatment (Figure 3). While there were differences between months for ABA normalized by fresh weight ($p = 0.03$), there was no difference between treatments ($p = 0.26$; Figure 2).

There was no significant difference in leaf mass per area between treatments ($p = 0.94$) or months ($p = 0.25$) (Figure 4). There was no significant difference between treatments for the turgor loss point ($p = 0.49$) (Figure 4) or any other pressure-volume curve trait (Supplemental Figure 6). There was no significant difference between treatments or months for mean vessel area per mm^2 ($p = 0.19$ and $p = 0.09$, respectively) or number of vessels per mm^2 ($p = 0.08$ and $p = 0.06$, respectively; Figure 4). While there were differences in non-structural carbohydrates among tissues and months, there were no differences between treatments (Figure 5).

Model simulations indicated that all trees in the drought treatment had a deeper effective water uptake depth as compared to the control treatment, except for the trees with the deepest effective water uptake depth of 6.6m ($p<0.001$; Figure 6; Supplemental Figure 5). Absolute differences in effective water uptake depth within each species between treatments ranged from 0 to 1.1m.

Discussion

Our goal was to test how the hydraulic and carbon-based traits of a diverse set of tropical rainforest trees responded to four years of experimental drought. The soil volumetric water content in the top

meter was significantly reduced by rainfall exclusion in the drought treatment (Figure 1; Tng et al., 2018). However, there were no differences in measured traits between the control and drought treatment, including predawn and midday water potentials (Figure 2), photosynthesis and stomatal conductance (Figure 2), foliar ABA level (Figure 2), leaf mass per area (Figure 4), turgor loss point (Figure 4), xylem vessel anatomy (Figure 4), and non-structural carbohydrates (Figure 5). The only empirically measured trait with a significant difference between treatments was intrinsic water use efficiency (A/g_s), but there was no difference in foliar stable carbon isotope ratios, which is a measure of integrated water use efficiency, between treatments (Figure 3). While the impact of drought on above-ground traits was surprisingly limited, results from our process-based photosynthetic gain and hydraulic cost optimization model suggest that trees shifted their effective water uptake depth to deeper soil layers in response to the drought treatment (Figure 6).

Typically, traits that respond to drought and regulate plant water use include stomatal conductance, water use efficiency, foliar turgor loss point, leaf phenology, and tolerance of low minimum seasonal tissue water potential (Bartlett et al., 2016; Blackman et al., 2019; Pivovaroff et al., 2016). For example, variable plant hydraulic conductance has previously been shown to control the seasonal plant water potential gradient in northern Australia (Franks et al., 2007). In our experiment, we saw homeostatic regulation of plant water status (Figure 2), even with a significant reduction in soil moisture in the upper soil layers between treatments (Figure 1), because of differences in the effective water uptake depth at deeper soil layers for trees in the drought treatment. This allowed trees to maintain water access (Figure 6) and therefore their water status. Tree plasticity for depth of water uptake has been shown for other tropical rainforest trees (Stahl et al., 2013). Our modeled differences in depth of effective water uptake fell well within the maximum rooting depth for tropical trees. For example, in a global review of maximum rooting depth, tropical evergreen forests had a maximum rooting depth of 7.3±2.8 m (Canadell et al., 1996). The deepest simulated effective water uptake depth for our trees was at 6.6 m, and within each species the absolute change in effective water uptake depth ranged from 0 to 1.1m between treatments (Figure 5). Further, Cheesman et al., 2020 found that at this study site the drought treatment had a significant effect on $\delta^{15}N$, which is likely a result of droughted trees shifting the depth of water access to deeper layers that also have an elevated $\delta^{15}N$. However, while we can manipulate the effective water uptake depth using the

photosynthetic gain and hydraulic cost optimization model (Sperry et al., 2017; Venturas et al., 2018), we cannot distinguish if this was, in fact, a change in the rooting depth of trees in the field *per se*, or if trees already had existing roots at that depth and they instead shifted the dominant depth from which they acquired water (Mackay et al., 2020). While this could be determined using stable water isotopes, the soil's rocky nature at this site (~32% rock by volume near the surface, and 44% below 0.2m depth; Liddell, 2015) makes that measurement technically challenging. Further, these results would be difficult to interpret as the isotopic gradient would differ between treatments. Besides, as we kept the above-ground biomass the same for each species' model across treatments, we cannot account for any allometric shifts between below and above-ground biomass (Mencuccini, 2003). Previous experiments have shown the leaf area index to decline in response to reduced plant-available water in the Amazonian tropics (Nepstad, 2002).

The homeostatic maintenance of tree water status across treatments also resulted in no difference in gas exchange, non-structural carbohydrates, or turgor loss point between treatments. Because of the differences in tree effective water uptake depth between treatments, the effective water supply to the trees and their leaves stayed the same. Without an impact on water supply and no experimental impact on the water demand (i.e. no change in vapor pressure deficit between treatments), these other traits were also maintained regardless of rainfall exclusion. Previous studies have also shown similar homeostatic trait maintenance patterns in tropical forests, including hydraulic traits (Pivovaroff et al., 2021) and non-structural carbohydrates (Dickman et al., 2019) across precipitation and water availability gradients. Furthermore, the lack of difference in turgor loss point between treatments indicates that trees were at equal hydraulic risk to reach wilting in both treatments (Figure 4). Hydraulic safety margins are generally thought of as an indicator of mortality risk, with species closer to or exceeding thresholds of water stress, including vulnerability to cavitation and turgor loss, being at greater risk of drought mortality (Anderegg et al., 2016; Choat et al., 2012). Previous research in moist tropical forests has shown that species with large hydraulic safety margins were protected against drought (Ziegler et al., 2019), while hydraulically vulnerable trees were killed during catastrophic drought (Powers et al., 2020). The homeostatic regulation of plant water status, gas exchange, non-structural carbohydrates, and other traits across treatments due to shifts in below-

ground dynamics suggests a potential below-ground mechanism to promote this forest's resistance to a decrease in rainfall.

Understanding how tropical forests respond to drought is essential for predicting climate change impact on tropical forest – atmosphere interactions. Many wet tropical forests have already experienced increased tree mortality rates, including the Amazon (Brienen et al., 2015; Hubau et al., 2020) and in Southeast Asia (Phillips et al., 2010). Our results, however, suggest that trees living on deep soils may be better adapted to surviving severe droughts that may arise in the future and therefore be more resilient to climate change. A resilient rainforest would serve as a refugia for flora and fauna in a rapidly changing world. However, more drastic changes in precipitation patterns or the interaction of multiple factors such as drought, rising temperature, and increased atmospheric demand (vapor pressure deficit) might still negatively impact these trees, especially for species that may be more moisture sensitive. For example, in a previous study at this site, the native palm *Normanbya normanbyi* had reduced photosynthetic rates, stomatal conductance, and even fruiting activity (Vogado et al., 2020) in response to the experimental drought treatment. This species tends to be shallower rooted than our study tree species and as a monocotyledon it is does not have secondary wood formation, disallowing sufficient acclimation to reduced soil moisture in the drought treatment. This warrants further empirical measurements of forest drought adaptation traits that are important for parameterizing predictive process based and Earth systems models.

Acknowledgments

We thank James Abend for essential assistance in the lab, Michele Schiffer for coordination of field trips and on-the-ground assistance at the Daintree Rainforest Observatory, and Andrew Thompson for operating the crane.

Funding

This research was supported as part of the Next Generation Ecosystem Experiments-Tropics, funded by the U.S. Department of Energy, Office of Science, Office of Biological and Environmental Research (Award #71073). The Daintree drought experiment has been supported by ARC grants (DP130104092 and FT130101319) to SL.

Data availability

All data is publicly available.

The QA/QC-ed raw LICOR gas exchange data are available on the NGEE-Tropics data archive: **Pivovaroff AL**, McDowell N, Jardine K, Barrozo T, Sampaio I, Souza D, Grossiord C, Cernusak L. (2021) Leaf gas exchange data, Nov 2018 and May 2019, Daintree Rainforest, Australia. NGEE-Tropics Data Archive. DOI: 10.15486/ngt/1773854

The QA/QC-ed raw foliar ABA, xylem anatomy, foliar d13C, LMA, leaf water potential, non-structural carbohydrates, and pressure volume curve parameters are available on the NGEE-Tropics data archive: **Pivovaroff AL**, McDowell N, Barrozo T, Brodribb T, Cernusak L, Grossiord C, Ishida Y, Jardine KJ, Laurance S, Leff R, Li W, Pacheco H, Sampaio I, Souza DC, Wang W, Zhang P. (2021) Functional trait data for 11 canopy tree species in the control and drought treatments at the Daintree Rainforest, Australia (AU-DRO) from the 2018 dry season and 2019 wet season. NGEE-Tropics Data Archive. DOI: 10.15486/ngt/1810164

The model code is available at (Leff, 2020).

The meteorological data are available from the Australia TERN Supersite (TERN, 2020).

The P_{50} and wood density values are available from (Peters et al., 2021).

Conflict of Interest

The authors declare no conflict of interest.

References

Anderegg, W. R. L., Klein, T., Bartlett, M. K., Sack, L., Pellegrini, A. F. A., & Choat, B. (2016). Meta-analysis reveals that hydraulic traits explain cross-species patterns of drought-induced tree

mortality across the globe. *Proceedings of the National Academy of Sciences*, *113*(18), 2–7. https://doi.org/10.1073/pnas.1525678113

Barbeta, A., Mejía-Chang, M., Ogaya, R., Voltas, J., Dawson, T. E., & Peñuelas, J. (2015). The combined effects of a long-term experimental drought and an extreme drought on the use of plant-water sources in a Mediterranean forest. *Global Change Biology*, *21*(3), 1213–1225. https://doi.org/10.1111/gcb.12785

Bartlett, M. K., Klein, T., Jansen, S., Choat, B., & Sack, L. (2016). The correlations and sequence of plant stomatal, hydraulic, and wilting responses to drought. *Proceedings of the National Academy of Sciences of the United States of America*, *113*(46), 13098–13103. https://doi.org/10.1073/pnas.1604088113

Blackman, C. J., Creek, D., Maier, C., Aspinwall, M. J., Drake, J. E., Pfautsch, S., O'Grady, A., Delzon, S., Medlyn, B. E., Tissue, D. T., Choat, B., & Meinzer, F. (2019). Drought response strategies and hydraulic traits contribute to mechanistic understanding of plant dry-down to hydraulic failure. *Tree Physiology*, *39*(6), 910–924. https://doi.org/10.1093/treephys/tpz016

Bouche, P. S., Larter, M., Domec, J. C., Burlett, R., Gasson, P., Jansen, S., & Delzon, S. (2014). A broad survey of hydraulic and mechanical safety in the xylem of conifers. *Journal of Experimental Botany*, *65*(15), 4419–4431. http://jxb.oxfordjournals.org/lookup/doi/10.1093/jxb/eru218

Brienen, R. J. W., Phillips, O. L., Feldpausch, T. R., Gloor, E., Baker, T. R., Lloyd, J., Lopez-Gonzalez, G., Monteagudo-Mendoza, A., Malhi, Y., Lewis, S. L., Vásquez Martinez, R., Alexiades, M., Álvarez Dávila, E., Alvarez-Loayza, P., Andrade, A., Aragao, L. E. O. C., Araujo-Murakami, A., Arets, E. J. M. M., Arroyo, L., … Zagt, R. J. (2015). Long-term decline of the Amazon carbon sink. *Nature*, *519*(7543), 344–348. https://doi.org/10.1038/nature14283

Canadell, J., Jackson, R. B. B., Ehleringer, J. R., Mooney, H. A. A., Sala, O. E. E., & Schulze, E. D. (1996). Maximum rooting depth of vegetation types at the global scale. *Oecologia*, *108*(4), 583–595.

Cheesman, A. W., Duff, H., Hill, K., Cernusak, L. A., & McInerney, F. A. (2020). Isotopic and morphologic proxies for reconstructing light environment and leaf function of fossil leaves: a modern calibration in the Daintree Rainforest, Australia. *American Journal of Botany*, *107*(8),

1165–1176. https://doi.org/10.1002/ajb2.1523

Choat, B., Brodribb, T. J., Brodersen, C. R., Duursma, R. A., López, R., & Medlyn, B. E. (2018). Triggers of tree mortality under drought. *Nature*, *558*(7711), 531–539. https://doi.org/10.1038/s41586-018-0240-x

Choat, B., Jansen, S., Brodribb, T. J., Cochard, H., Delzon, S., Bhaskar, R., Bucci, S. J., Feild, T. S., Gleason, S. M., Hacke, U. G., Jacobsen, A. L., Lens, F., Maherali, H., Martínez-Vilalta, J., Mayr, S., Mencuccini, M., Mitchell, P. J., Nardini, A., Pittermann, J., … Zanne, A. E. (2012). Global convergence in the vulnerability of forests to drought. *Nature*, *491*(7426), 752–755. http://dx.doi.org/10.1038/nature11688

Crausbay, S. D., Ramirez, A. R., Carter, S. L., Cross, M. S., Hall, K. R., Bathke, D. J., Betancourt, J. L., Colt, S., Cravens, A. E., Dalton, M. S., Dunham, J. B., Hay, L. E., Hayes, M. J., McEvoy, J., McNutt, C. A., Moritz, M. A., Nislow, K. H., Raheem, N., & Sanford, T. (2017). Defining ecological drought for the twenty-first century. *Bulletin of the American Meteorological Society*, *98*(12), 2543–2550. https://doi.org/10.1175/BAMS-D-16-0292.1

Cuddington, K., Fortin, M. J., Gerber, L. R., Hastings, A., Liebhold, A., O'connor, M., & Ray, C. (2013). Process-based models are required to manage ecological systems in a changing world. *Ecosphere*, *4*(2), 1–12. https://doi.org/10.1890/ES12-00178.1

da Costa, A. C. L., Galbraith, D., Almeida, S., Portela, B. T. T., da Costa, M., de Athaydes Silva Junior, J., Braga, A. P., de Gonçalves, P. H. L., de Oliveira, A. A., Fisher, R., Phillips, O. L., Metcalfe, D. B., Levy, P., & Meir, P. (2010). Effect of 7 yr of experimental drought on vegetation dynamics and biomass storage of an eastern Amazonian rainforest. *New Phytologist*, *187*(3), 579–591. https://doi.org/10.1111/j.1469-8137.2010.03309.x

David, T. S., Henriques, M. O., Kurz-Besson, C., Nunes, J., Valente, F., Vaz, M., Pereira, J. S., Siegwolf, R., Chaves, M. M., Gazarini, L. C., & David, J. S. (2007). Water-use strategies in two co-occurring Mediterranean evergreen oaks: Surviving the summer drought. *Tree Physiology*, *27*(6), 793–803. https://doi.org/10.1093/treephys/27.6.793

Dickman, L. T., McDowell, N. G., Grossiord, C., Collins, A. D., Wolfe, B. T., Detto, M., Wright, S. J., Medina-Vega, J. A., Goodsman, D., Rogers, A., Serbin, S. P., Wu, J., Ely, K. S., Michaletz, S. T., Xu, C., Kueppers, L., & Chambers, J. Q. (2019). Homoeostatic maintenance of nonstructural

carbohydrates during the 2015–2016 El Niño drought across a tropical forest precipitation gradient. *Plant Cell and Environment*, *42*(5), 1705–1714. https://doi.org/10.1111/pce.13501

Domec, J. C., & Gartner, B. L. (2002). Age- and position-related changes in hydraulic versus mechanical dysfunction of xylem: Inferring the design criteria for Douglas-fir wood structure. *Tree Physiology*, *22*(2–3), 91–104. https://doi.org/10.1093/treephys/22.2-3.91

Duursma, R. A. (2015). Plantecophys - An R package for analysing and modelling leaf gas exchange data. *PLoS ONE*, *10*(11), 1–13. https://doi.org/10.1371/journal.pone.0143346

Duursma, R., & Choat, B. (2017). fitplc - an R package to fit hydraulic vulnerability curves. *Journal of Plant Hydraulics*, *4*(0), 002. https://doi.org/10.20870/jph.2017.e002

Eggemeyer, K. D., Awada, T., Harvey, F. E., Wedin, D. A., Zhou, X., & Zanner, C. W. (2009). Seasonal changes in depth of water uptake for encroaching trees Juniperus virginiana and Pinus ponderosa and two dominant C4 grasses in a semiarid grassland. *Tree Physiology*, *29*(2), 157–169. https://doi.org/10.1093/treephys/tpn019

Farquhar, G. D., & von Caemmerer, S. (1980). A Biochemical Model of Photosynthetic CO2 Assimilation in Leaves of C3 Species. *Planta*, *149*, 78–90. papers3://publication/uuid/18A39B28-F971-4220-902E-2775356FCD8C

Franks, P. J., Drake, P. L., & Froend, R. H. (2007). Anisohydric but isohydrodynamic: Seasonally constant plant water potential gradient explained by a stomatal control mechanism incorporating variable plant hydraulic conductance. *Plant, Cell and Environment*, *30*(1), 19–30. https://doi.org/10.1111/j.1365-3040.2006.01600.x

Hammond, W. M., Yu, K., Wilson, L. A., Will, R. E., Anderegg, W. R. L., & Adams, H. D. (2019). Dead or dying? Quantifying the point of no return from hydraulic failure in drought-induced tree mortality. *New Phytologist*. https://doi.org/10.1111/nph.15922

Hoch, G., Popp, M., & Körner, C. (2002). Altitudinal increase of mobile carbon pools in Pinus cembra suggests sink limitation of growth at the Swiss treeline. *Oikos*, *98*(3), 361–374. https://doi.org/10.1034/j.1600-0706.2002.980301.x

Hubau, W., Lewis, S. L., Phillips, O. L., Affum-Baffoe, K., Beeckman, H., Cuní-Sanchez, A., Daniels, A. K., Ewango, C. E. N., Fauset, S., Mukinzi, J. M., Sheil, D., Sonké, B., Sullivan, M. J. P., Sunderland, T. C. H., Taedoumg, H., Thomas, S. C., White, L. J. T., Abernethy, K. A., Adu-

Bredu, S., … Zemagho, L. (2020). Asynchronous carbon sink saturation in African and Amazonian tropical forests. *Nature*, *579*(7797), 80–87. https://doi.org/10.1038/s41586-020-2035-0

Johnson, D. M., Domec, J. C., Carter Berry, Z., Schwantes, A. M., McCulloh, K. A., Woodruff, D. R., Wayne Polley, H., Wortemann, R., Swenson, J. J., Scott Mackay, D., McDowell, N. G., & Jackson, R. B. (2018). Co-occurring woody species have diverse hydraulic strategies and mortality rates during an extreme drought. *Plant Cell and Environment*, *41*(3), 576–588. https://doi.org/10.1111/pce.13121

Klein, T., Rotenberg, E., Cohen-Hilaleh, E., Raz-Yaseef, N., Tatarinov, F., Preisler, Y., Ogée, J., Cohen, S., & Yakir, D. (2014). Quantifying transpirable soil water and its relations to tree water use dynamics in a water-limited pine forest. *Ecohydrology*, *7*(2), 409–419. https://doi.org/10.1002/eco.1360

Laidlaw, M., Kitching, R., Goodall, K., Small, A., & Stork, N. (2007). Temporal and spatial variation in an Australian tropical rainforest. *Austral Ecology*, *32*(1), 10–20. https://doi.org/10.1111/j.1442-9993.2007.01739.x

Landhäusser, S. M., Chow, P. S., Turin Dickman, L., Furze, M. E., Kuhlman, I., Schmid, S., Wiesenbauer, J., Wild, B., Gleixner, G., Hartmann, H., Hoch, G., McDowell, N. G., Richardson, A. D., Richter, A., & Adams, H. D. (2018). Standardized protocols and procedures can precisely and accurately quantify non-structural carbohydrates. *Tree Physiology*, *38*(12), 1764–1778. https://doi.org/10.1093/treephys/tpy118

Leff, R. (2020). *ezSperry-beta*. https://github.com/RileyLeff/ezSperry-beta

Liddell, M. J. (2015). *Soil Pit Data, Soil Characterisation, Far North Queensland Rainforest SuperSite, Daintree Rainforest Observatory, Cape Tribulation, 2006, Version 5*. TERN Australian SuperSite Network. http://supersites.tern.org.au/knb/metacat/supersite.64/html

Liddell, M. J., & Laurance, S. (2015). *Leaf Area Index Data, Far North Queensland Rainforest SuperSite, Daintree Rainforest Observatory, Cape Tribulation, Core 1 ha, 2014*. TERN Australian SuperSite Network. http://supersites.tern.org.au/knb/metacat/supersite.238.13/html

Love, D. M., Venturas, M. D., Sperry, J. S., Brooks, P. D., Pettit, J. L., Wang, Y., Anderegg, W. R. L., Tai, X., & Mackay, D. S. (2019). Dependence of Aspen Stands on a Subsurface Water

Subsidy: Implications for Climate Change Impacts. *Water Resources Research*, *55*(3), 1833–1848. https://doi.org/10.1029/2018WR023468

Mackay, D. S., Savoy, P. R., Grossiord, C., Tai, X., Pleban, J. R., Wang, D. R., McDowell, N. G., Adams, H. D., & Sperry, J. S. (2020). Conifers depend on established roots during drought: results from a coupled model of carbon allocation and hydraulics. *New Phytologist*, *225*(2), 679–692. https://doi.org/10.1111/nph.16043

McAdam, S. A. (2015). Physiochemical quantification of Abscisic Acid levels in plant tissues with an added internal standard by ultra-performance liquid chromatography. *Bio-Protocol*, *5*(18), e1599. https://doi.org/10.21769/BioProtoc.1599

McAdam, S. A., & Brodribb, T. J. (2014). Separating active and passive influences on stomatal control of transpiration. *Plant Physiology*, *164*(4), 1578–1586. https://doi.org/10.1104/pp.113.231944

McDowell, N. G., Allen, C. D., Anderson-teixeira, K., Aukema, B. H., Bond-lamberty, B., Chini, L., Clark, J. S., Dietze, M., Grossiord, C., Hanbury-brown, A., Hurtt, G. C., Jackson, R. B., Johnson, D. J., Kueppers, L., Lichstein, J. W., Ogle, K., Poulter, B., Pugh, T. A. M. M., Seidl, R., … Xu, C. (2020). Pervasive shifts in forest dynamics in a changing world. *Science*, *368*(964), eaaz9463. https://doi.org/10.1126/science.aaz9463

McDowell, N. G., Beerling, D. J., Breshears, D. D., Fisher, R. A., Raffa, K. F., & Stitt, M. (2011). The interdependence of mechanisms underlying climate-driven vegetation mortality. *Trends in Ecology & Evolution*, *26*(10), 523–532. http://eutils.ncbi.nlm.nih.gov/entrez/eutils/elink.fcgi?dbfrom=pubmed&id=21802765&retmode=ref&cmd=prlinks

Meir, P., Brando, P. M., Nepstad, D., Vasconcelos, S., Costa, A. C. L., Davidson, E., Almeida, S., Fisher, R. A., Sotta, E. D., Zarin, D., & Cardinot, G. (2009). The Effects of Drought on Amazonian Rain Forests. *Amazonia and Global Change*, 429–449. https://doi.org/10.1029/2009GM000882

Meir, Patrick, Mencuccini, M., & Dewar, R. C. (2015). *Drought-related tree mortality : addressing the gaps in understanding and prediction*.

Meir, Patrick, & Woodward, F. I. (2010). Amazonian rain forests and drought: Response and

vulnerability. *New Phytologist*, *187*(3), 553–557. https://doi.org/10.1111/j.1469-8137.2010.03390.x

Mencuccini, M. (2003). The ecological significance of long-distance water transport: Short-term regulation, long-term acclimation and the hydraulic costs of stature across plant life forms. *Plant, Cell and Environment*, *26*(1), 163–182. https://doi.org/10.1046/j.1365-3040.2003.00991.x

Nepstad, D. C. (2002). The effects of partial throughfall exclusion on canopy processes, aboveground production, and biogeochemistry of an Amazon forest. *Journal of Geophysical Research*, *107*(D20), 1–18. https://doi.org/10.1029/2001jd000360

Peters, J. M. R., López, R., Nolf, M., Hutley, L. B., Wardlaw, T., Cernusak, L. A., & Choat, B. (2021). Living on the edge: A continental-scale assessment of forest vulnerability to drought. *Global Change Biology*, *January*, 1–22. https://doi.org/10.1111/gcb.15641

Phillips, O. L., Heijden, G. Van Der, Lewis, S. L., Lo, G., Lloyd, J., Malhi, Y., Monteagudo, A., Almeida, S., Da, E. A., Andelman, S., Andrade, A., Arroyo, L., Aymard, G., Baker, T. R., Costa, L., Feldpausch, T. R., Fisher, J. B., Fyllas, N. M., Freitas, M. A., … Vilanova, E. (2010). Drought–mortality relationships for tropical forests. *New Phytologist*, *187*, 631–646.

Pivovaroff, A. L., Pasquini, S. C., De Guzman, M. E., Alstad, K. P., Stemke, J. S., & Santiago, L. S. (2016). Multiple strategies for drought survival among woody plant species. *Functional Ecology*, *30*(4), 517–526. https://doi.org/10.1111/1365-2435.12518

Pivovaroff, A. L., Wolfe, B. T., McDowell, N., Christoffersen, B., Davies, S., Dickman, L. T., Grossiord, C., Leff, R. T., Rogers, A., Serbin, S. P., Wright, S. J., Wu, J., Xu, C., & Chambers, J. Q. (2021). Hydraulic architecture explains species moisture dependency but not mortality rates across a tropical rainfall gradient. *Biotropica*, *March*, 1–13. https://doi.org/10.1111/btp.12964

Powers, J. S., Vargas G., G., Brodribb, T. J., Schwartz, N. B., Pérez-Aviles, D., Smith-Martin, C. M., Becknell, J. M., Aureli, F., Blanco, R., Calderón-Morales, E., Calvo-Alvarado, J. C., Calvo-Obando, A. J., Chavarría, M. M., Carvajal-Vanegas, D., Jiménez-Rodríguez, C. D., Murillo Chacon, E., Schaffner, C. M., Werden, L. K., Xu, X., & Medvigy, D. (2020). A catastrophic tropical drought kills hydraulically vulnerable tree species. *Global Change Biology*, *26*(5), 3122–3133. https://doi.org/10.1111/gcb.15037

Poyatos, R., Aguadé, D., & Martínez-Vilalta, J. (2018). Below-ground hydraulic constraints during

drought-induced decline in Scots pine. *Annals of Forest Science*, *75*(4). https://doi.org/10.1007/s13595-018-0778-7

R Core Team. (2020). *R: A language and environment for statistical computing*. R Foundation for Statistical Computing. https://www.r-project.org/

Rossatto, D. R., de Carvalho Ramos Silva, L., Villalobos-Vega, R., Sternberg, L. da S. L., & Franco, A. C. (2012). Depth of water uptake in woody plants relates to groundwater level and vegetation structure along a topographic gradient in a neotropical savanna. *Environmental and Experimental Botany*, *77*, 259–266. https://doi.org/10.1016/j.envexpbot.2011.11.025

RStudio Team. (2020). *RStudio: Integrated Development for R*. RStudio, PBC, Boston, MA. http://www.rstudio.com/

Snyder, K. A., & Williams, D. G. (2003). Defoliation alters water uptake by deep and shallow roots of Prosopis velutina (Velvet Mesquite). *Functional Ecology*, *17*(3), 363–374. https://doi.org/10.1046/j.1365-2435.2003.00739.x

Sperry, J. S., & Love, D. M. (2015). *What plant hydraulics can tell us about responses to climate-change droughts*.

Sperry, J. S., Venturas, M. D., Anderegg, W. R. L., Mencuccini, M., Mackay, D. S., Wang, Y., & Love, D. M. (2017). Predicting stomatal responses to the environment from the optimization of photosynthetic gain and hydraulic cost. *Plant Cell and Environment*, *40*(6), 816–830. https://doi.org/10.1111/pce.12852

Sperry, J. S., Wang, Y., Wolfe, B. T., Mackay, D. S., Anderegg, W. R. L., Mcdowell, N. G., & Pockman, W. T. (2016). Pragmatic hydraulic theory predicts stomatal responses to climatic water deficits. *New Phytologist*, 577–589. https://doi.org/10.1111/nph.14059

Stahl, C., Hérault, B., Rossi, V., Burban, B., Bréchet, C., & Bonal, D. (2013). Depth of soil water uptake by tropical rainforest trees during dry periods: Does tree dimension matter? *Oecologia*, *173*(4), 1191–1201. https://doi.org/10.1007/s00442-013-2724-6

TERN. (2020). *TERN Daintree Rainforest SuperSite*. https://www.tern.org.au/tern-observatory/tern-ecosystem-processes/daintree-rainforest-supersite/

Tng, D. Y. P., Apgaua, D. M. G., Campbell, M. J., Cox, C. J., Crayn, D. M., Ishida, F. Y., Laidlaw, M. J., Liddell, M. J., Seager, M., & Laurance, S. G. W. (2016). Vegetation and floristics of a

lowland tropical rainforest in northeast Australia. *Biodiversity Data Journal*, *4*(1), 1–20. https://doi.org/10.3897/BDJ.4.e7599

Tng, D. Y. P., Apgaua, D. M. G., Ishida, Y. F., Mencuccini, M., Lloyd, J., Laurance, W. F., & Laurance, S. G. W. (2018). Rainforest trees respond to drought by modifying their hydraulic architecture. *Ecology and Evolution*, *8*(24), 12479–12491. https://doi.org/10.1002/ece3.4601

Trenberth, K. E., Dai, A., Van Der Schrier, G., Jones, P. D., Barichivich, J., Briffa, K. R., & Sheffield, J. (2014). Global warming and changes in drought. *Nature Climate Change*, *4*(1), 17–22. https://doi.org/10.1038/nclimate2067

van Genuchten, M. T. (1980). A closed-form equation for predicting the hydraulic conductivity of unsaturated soils. *Soil Science Society of America Journal*, *44*(5), 892–898.

Vargas, G. (2019). *Pressure Volume Curves*. https://github.com/gevargu/Plant_Ecophysiology_Tools/tree/master/Pressure Volume Curves

Venturas, M. D., Sperry, J. S., Love, D. M., Frehner, E. H., Allred, M. G., Wang, Y., & Anderegg, W. R. L. (2018). A stomatal control model based on optimization of carbon gain versus hydraulic risk predicts aspen sapling responses to drought. *New Phytologist*, *220*(3), 836–850. https://doi.org/10.1111/nph.15333

Vogado, N. O., Liddell, M. J., Laurance, S. G. W., Campbell, M. J., Cheesman, A. W., Engert, J. E., Palma, A. C., Ishida, F. Y., & Cernusak, L. A. (2020). The effects of an experimental drought on the ecophysiology and fruiting phenology of a tropical rainforest palm. *Journal of Plant Ecology*. https://doi.org/10.1093/jpe/rtaa069

Voltas, J., Lucabaugh, D., Chambel, M. R., & Ferrio, J. P. (2015). Intraspecific variation in the use of water sources by the circum-Mediterranean conifer Pinus halepensis. *New Phytologist*, *208*(4), 1031–1041. https://doi.org/10.1111/nph.13569

Zhou, L., Tian, Y., Myneni, R. B., Ciais, P., Saatchi, S., Liu, Y. Y., Piao, S., Chen, H., Vermote, E. F., Song, C., & Hwang, T. (2014). Widespread decline of Congo rainforest greenness in the past decade. *Nature*, *508*(7498), 86–90. https://doi.org/10.1038/nature13265

Ziegler, C., Coste, S., Stahl, C., Delzon, S., Levionnois, S., Cazal, J., Cochard, H., Esquivel-Muelbert, A., Goret, J. Y., Heuret, P., Jaouen, G., Santiago, L. S., & Bonal, D. (2019). Large hydraulic safety margins protect Neotropical canopy rainforest tree species against hydraulic failure during

drought. *Annals of Forest Science*, *76*(4). https://doi.org/10.1007/s13595-019-0905-0

Figure captions.

Figure 1. Daily total rainfall (mm), daily mean air temperature (℃), and daily mean soil volumetric water content for the control (purple) and drought (yellow) treatment at four different depths (10cm, 50cm, 100cm, and 150cm) measured at the Daintree Rainforest Observatory in Australia in 2018.

Figure 2. Predawn and midday water potentials, photosynthesis, stomatal conductance, intrinsic water use efficiency (*A*/*g*s), and foliar abscisic acid (ABA) levels measured on 11 tree species between control (purple) and drought (yellow) treatments during the wet and dry season at the Daintree Rainforest Observatory in Australia. The boxplots display the median as a bold horizontal line, with colored hinges above and below the median to illustrate the 25th and 75th percentile. Outliers, values more than 1.5 times the inter-quartile range, are displayed as individual black points. The raw data points are overlaid on the boxplots as shaded points. For the ABA level panel, the y-axis is scaled in that 3 outliers above 20,000 ng g-1 have been excluded. Within each panel, different letters indicate a statistically significant difference ($p<0.05$).

Figure 3. Foliar $\delta^{13}C$ measured on 11 tree species between control (purple) and drought (yellow) treatments during the wet and dry season at the Daintree Rainforest Observatory in Australia. The right panel shows foliar $\delta^{13}C$ measured on a subset of 5 species from the original 11 that were resampled for replication (n=3) to determine if there were within species differences between treatments. The boxplots display the median as a bold horizontal line, with colored hinges above and below the median to illustrate the 25th and 75th percentile. Outliers, values more than 1.5 times the inter-quartile range, are displayed as individual black points. The raw data points are overlaid on the boxplots as shaded points. Within each panel, different letters indicate a statistically significant difference ($p<0.05$).

Figure 4. Leaf mass per area, turgor loss point, mean vessel area per mm^2, and number of vessels per mm^2 measured on 11 tree species between control (purple) and drought (yellow) treatments during the wet and dry season at the Daintree Rainforest Observatory in Australia. The boxplots display the median as a bold horizontal line, with colored hinges above and below the median to illustrate the

25th and 75th percentile. Outliers, values more than 1.5 times the inter-quartile range, are displayed as individual black points. The raw data points are overlaid on the boxplots as shaded points. Within each panel, different letters indicate a statistically significant difference ($p<0.05$).

Figure 5. Non-structural carbohydrates, including total sugars (glucose, fructose, and sucrose), starch, and total non-structural carbohydrates (starch plus all sugars), measured on 11 tree species between control (purple) and drought (yellow) treatments during the wet and dry season at the Daintree Rainforest Observatory in Australia. The boxplots display the median as a bold horizontal line, with colored hinges above and below the median to illustrate the 25th and 75th percentile. Outliers, values more than 1.5 times the inter-quartile range, are displayed as individual black points. The raw data points are overlaid on the boxplots as shaded points. Within each panel, different letters indicate a statistically significant difference ($p<0.05$).

Figure 6. Modeled effective water uptake depth for 8 tree species between the control and drought treatment at the Daintree Rainforest in Australia. We could only model 8 of the original 11 study species because it was not possible to conduct vulnerability curves for 3 of the species due to excessive latex and mucilage in the stems.

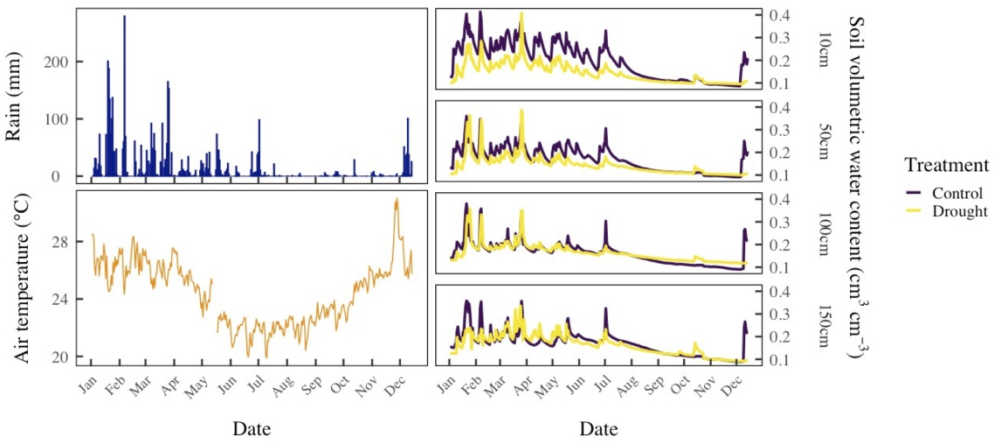

gcb_15869_f1.jpg

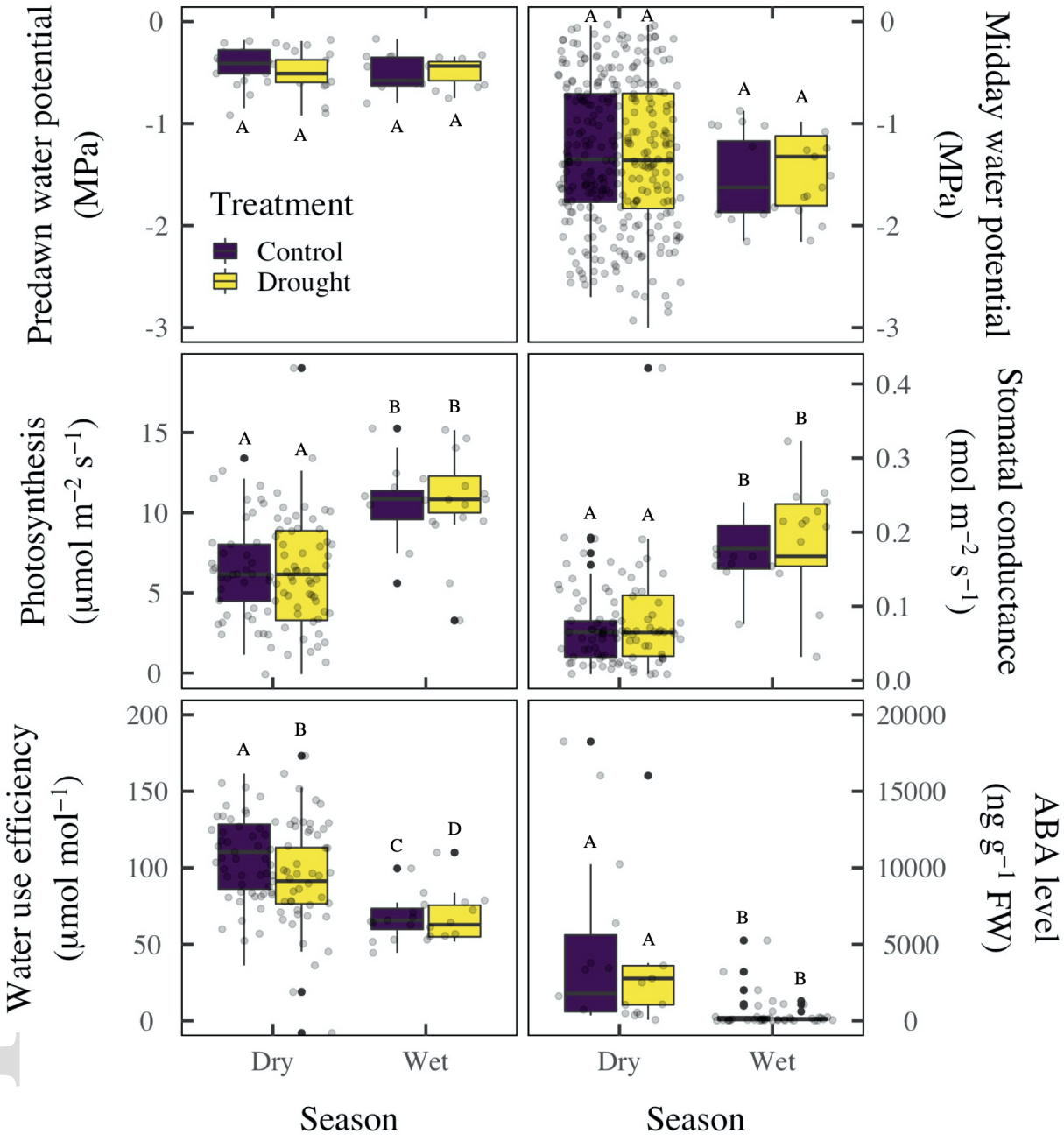

gcb_15869_f2.jpg

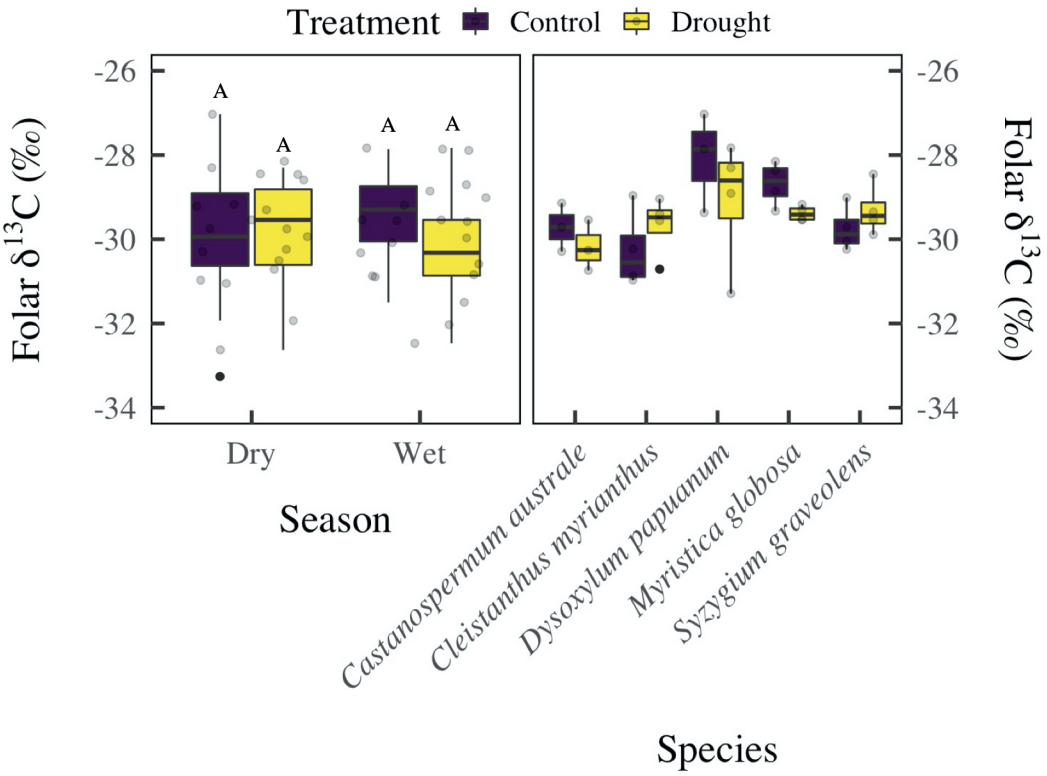

gcb_15869_f3.jpg

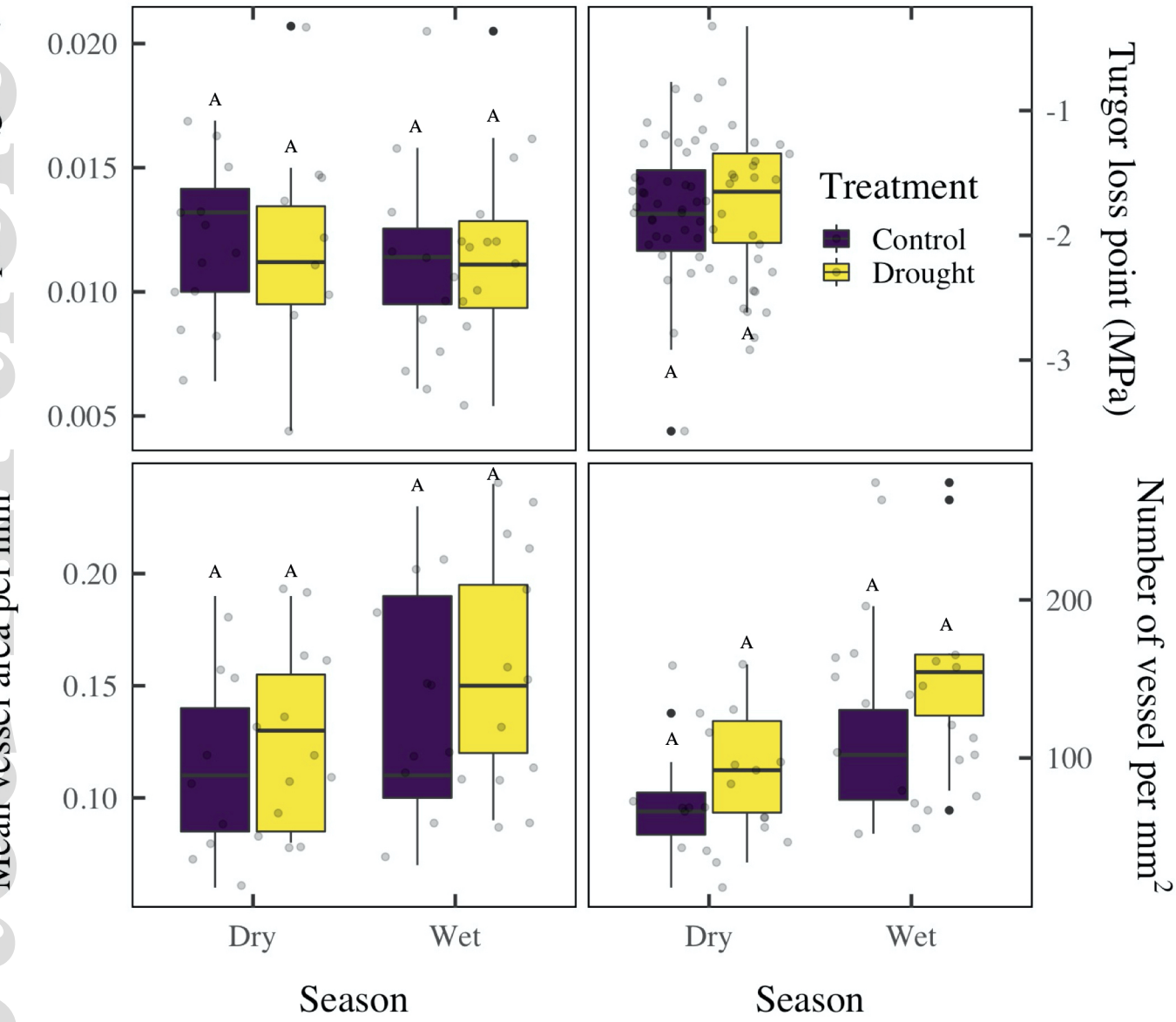

gcb_15869_f4.jpg

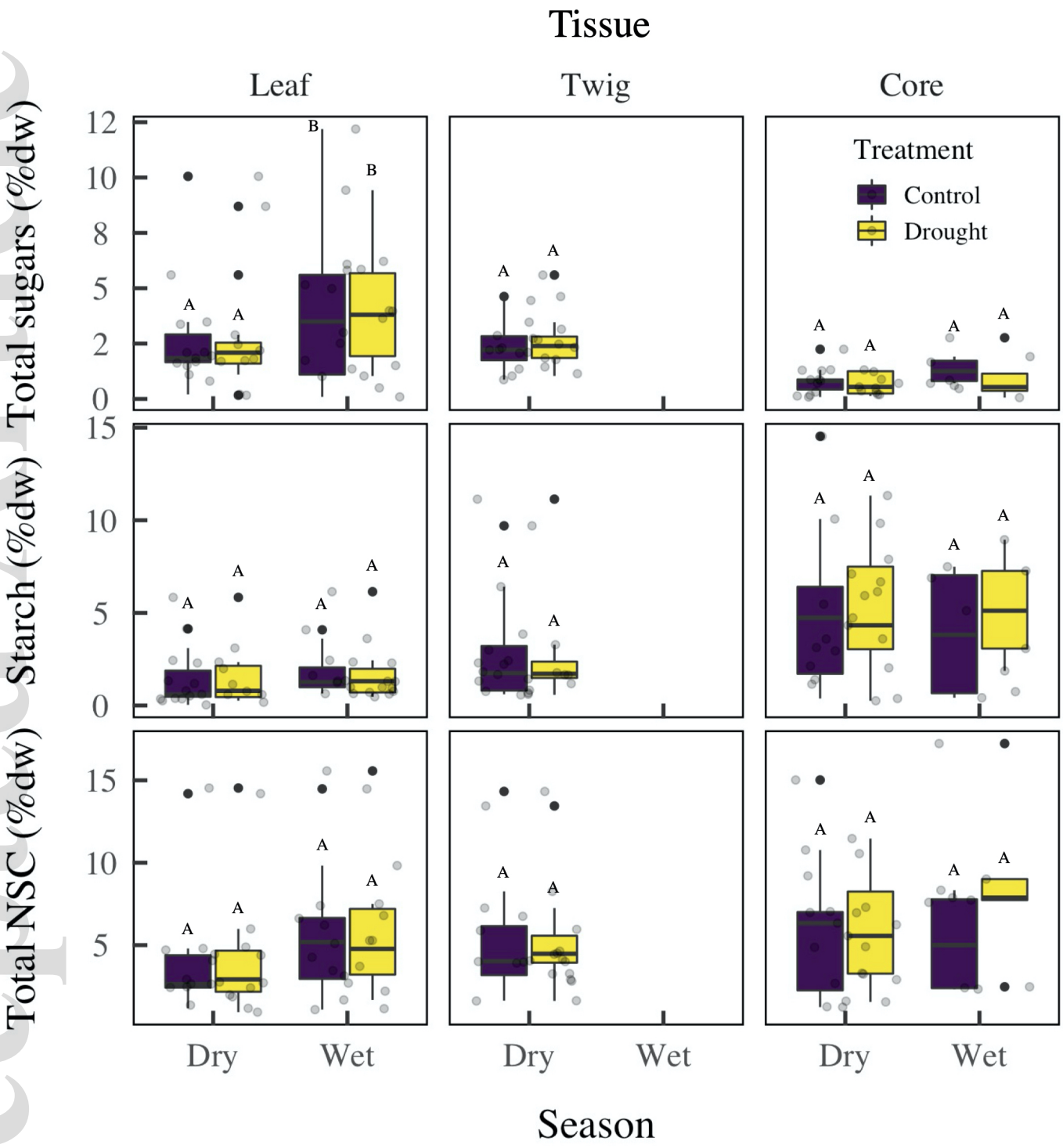

gcb_15869_f5.jpg

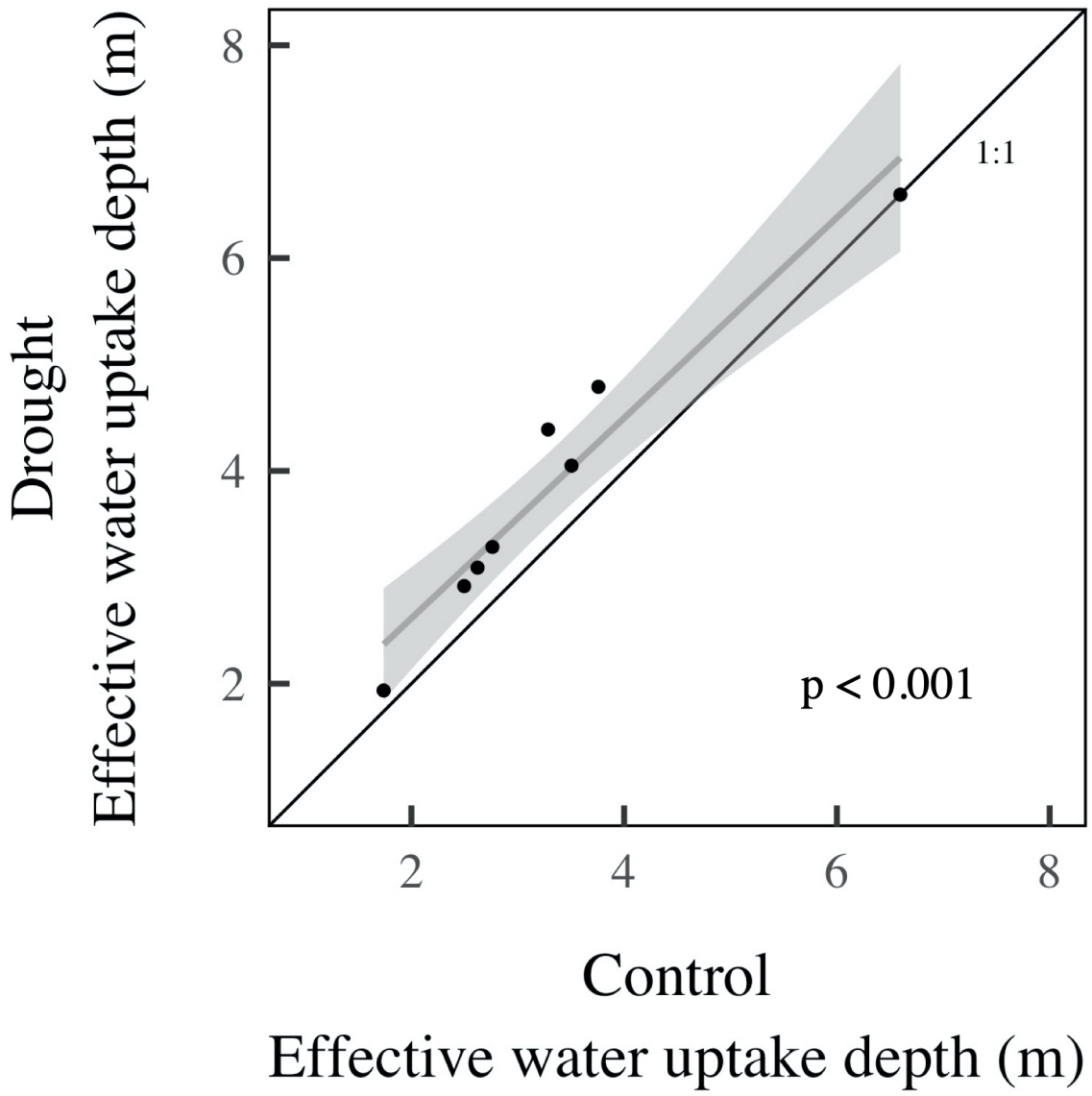

gcb_15869_f6.jpg